JACC: CARDIOVASCULAR IMAGING VOL. 7, NO. 5, 2014

ISSN 1936-878X/$36.00
PUBLISHED BY ELSEVIER INC. http://dx.doi.org/10.1016/j.jcmg.2014.03.002

Noninvasive Risk Stratification of Patients With Transthyretin Amyloidosis

Arnt V. Kristen, MD,* Katrin Scherer, MS,* Sebastian Buss, MD,*
Fabian aus dem Siepen, MS,* Sabine Haufe, MD,† Ralf Bauer, MD,*
Katrin Hinderhofer, PhD,‡ Evangelos Giannitsis, MD,* Stefan Hardt, MD,*
Uwe Haberkorn, MD,† Hugo A. Katus, MD,* Henning Steen, MD*

Heidelberg, Germany

OBJECTIVES We sought to evaluate noninvasive parameters by electrocardiography, echocardiography, technetium-99m–3,3-diphosphono-1,2-propanodicarboxylic acid (^{99m}Tc-DPD) scintigraphy, and cardiac magnetic resonance for the prediction of all-cause mortality in patients with cardiac transthyretin amyloidosis (ATTR).

BACKGROUND ATTR may present with highly variable symptoms, including polyneuropathy and cardiomyopathy, the latter being associated with a poor outcome. However, data on noninvasive risk stratification of ATTR are limited.

METHODS A total of 70 patients with ATTR were evaluated by echocardiography, cardiac biomarkers, and ^{99m}Tc-DPD scintigraphy. Cardiac magnetic resonance was performed in 30 patients. Echocardiographic findings and plasma levels of biomarkers were correlated with results of quantitative analysis of scintigraphy using a region-of-interest technique (whole-body as well as heart tracer retention). Receiver-operating characteristic (ROC) analysis was performed to calculate a cutoff value of ^{99m}Tc-DPD scintigraphy for heart retention for the diagnosis of cardiac amyloid involvement with the highest sensitivity and specificity. Univariate and multivariate analyses were performed in patients with cardiac involvement ($n = 60$) to determine noninvasive predictors of all-cause mortality.

RESULTS Scintigraphy findings correlated with morphological (interventricular septum thickness, left ventricular hypertrophy index) as well as functional (mitral annular systolic velocity, mitral/tricuspid annular plane systolic excursion) findings, cardiac biomarkers, renal function, and late gadolinium enhancement. The ROC-derived cutoff for the detection of cardiac amyloidosis by scintigraphic heart tracer retention was 4.8%. Univariate Cox regression revealed N-terminal pro–B-type natriuretic peptide, troponin T, mitral annular plane systolic excursion, and left ventricular hypertrophy index as predictors of all-cause mortality. However, on multivariate analysis, troponin T remained the only independent predictor of survival. The ROC-derived cutoff value of troponin T predicting all-cause mortality with the highest sensitivity (80.0%) and specificity (68.7%) was 0.0375 ng/l.

CONCLUSIONS Quantitative analysis of tracer retention is capable of characterizing the severity of cardiac involvement in ATTR. By multivariate analysis, troponin T remained the only independent predictor of survival. (J Am Coll Cardiol Img 2014;7:502–10) © 2014 by the American College of Cardiology Foundation

From the *Department of Cardiology, Angiology, and Respiratory Medicine, University Hospital Heidelberg, Heidelberg, Germany; †Department of Nuclear Medicine, University Hospital Heidelberg, Heidelberg, Germany; and the ‡Institute of Human Genetics, University Hospital Heidelberg, Heidelberg, Germany. Dr. Giannitsis has received research support and honoraria from Roche Diagnostics. Dr. Katus has developed the cTNT assay and holds a joint patent with Roche Diagnostics, Germany; and he has received research support and honoraria for lectures from Roche Diagnostics. All other authors have reported that they have no relationships relevant to the contents of this paper to disclose.

Manuscript received January 22, 2014; revised manuscript received March 7, 2014, accepted March 11, 2014.

Human transthyretin (TTR) is the amyloid precursor protein in transthyretin amyloidosis (ATTR). TTR usually forms a tetramer that is capable of binding thyroxine, whereas the monomeric form, which is rich in beta sheets, readily forms amyloid fibrils. More than 100 TTR point mutants are known to be amyloidogenic including the most common mutation, Val30Met (substitution of methionine for valine at position 30) (1).

See page 511

Depending on the specific genotype, sex, endemic area, and composition of amyloid fibrils (2,3), they predispose to the development of a preferentially sensorimotor polyneuropathy (TTR familial amyloidotic polyneuropathy) and/or (restrictive) cardiomyopathy (transthyretin familial amyloidotic cardiomyopathy [TTR-FAC]) (4–9). Moreover, cardiac deposition of wild-type TTR amyloid is a common aging phenomenon named senile systemic amyloidosis (SSA) (10) that is found in 25% of post-mortem cardiac biopsy specimens from patients older than 85 years of age. It is predominantly characterized by symptoms of heart failure.

Cardiac involvement represents the major complication of ATTR, either of the hereditary or wild type (2,9,11), even though the median survival of patients with ATTR appears to be much better than that of individuals with light-chain amyloidosis (12). At present, clinical variables that are potentially useful for assessment of disease severity and prognosis in ATTR patients are not elucidated in detail (13–18).

Technetium-99m–3,3-diphosphono-1,2-propanodicarboxylic acid (^{99m}Tc-DPD) scintigraphy is a well standardized and widely available technique for skeletal imaging. Recently, it was demonstrated as a tool for noninvasive imaging of cardiac amyloid deposits in patients with ATTR, yielding a high diagnostic sensitivity (19). Minor tracer retention can be found in patients with advanced cardiac light-chain amyloidosis (20). The clinical value of ^{99m}Tc-DPD for prediction of outcome in ATTR has not been evaluated in detail (21). Thus, the impact of clinical, electrocardiographic, echocardiographic, scintigraphic, and cardiac magnetic resonance (CMR) variables for risk stratification were investigated in patients with ATTR.

METHODS

Between September 2005 and July 2012, 70 consecutive patients (53 male, 17 female; mean age 62.1 ± 2.1 years) with ATTR (TTR-FAC: n = 36; SSA: n = 34) were evaluated at the outpatient department of Heidelberg Amyloidosis Center, Heidelberg, Germany. All patients had biopsy-proven ATTR (heart: n = 53; rectum: n = 10; abdominal fat: n = 3; nerve: n = 3; and urinary bladder: n = 1). Amyloid was confirmed by green birefringence of Congo red–stained sections viewed in polarized light and characterized by immunohistological staining. All patients underwent screening for hereditary ATTR by isoelectric focusing of serum and sequencing of genomic deoxyribonucleic acid after a written informed consent was obtained (22). Furthermore, a serum/urine immunofixation electrophoresis and a serum-free light-chain test were performed. If both a clonal light-chain and a mutant TTR were excluded, a diagnosis of SSA was made. All patients were evaluated by echocardiography with Doppler studies, ^{99m}Tc-DPD scintigraphy, and standard blood tests including N-terminal pro–B-type natriuretic peptide (NT-proBNP) (Elecsys proBNP, Roche Diagnostics, Mannheim, Germany) as well as troponin T (fourth-generation assay, Elecsys Troponin T, Roche Diagnostics). CMR was performed in 30 of 70 patients.

Cardiac involvement was defined as a cardiac biopsy specimen containing amyloid or by myocardial wall thickening on an echocardiogram in the absence of any history of arterial hypertension or valvular heart disease in patients with extracardiac amyloidosis proven by positive Congo red staining of any tissue specimen. Follow-up for analysis of all-cause mortality was done either by a personal visit to or other forms of communication with the Heidelberg Amyloidosis Center (n = 48). If no follow-up information was available for at least 3 months (n = 19), a telephone call was made at the end of the observation period (July 31, 2013). Three of these patients were lost during follow-up.

Echocardiography. All transthoracic echocardiographic imaging was performed by experienced investigators using a commercially available ultrasound machine (Vivid 7, GE Healthcare, Milwaukee, Wisconsin). Morphological and functional evaluation of cardiac chambers was performed according to the recommendations of the American Society of Echocardiography (23–26). Left ventricular (LV) ejection fraction was calculated by the modified Simpson method (25) and was considered markedly impaired if it was <40%. All recordings

ABBREVIATIONS AND ACRONYMS

ATTR = transthyretin amyloidosis

CMR = cardiac magnetic resonance

eGFR = estimated glomerular filtration rate

HR = heart, sternum, and thoracic spine tracer retention

LV = left ventricular

NT-proBNP = N-terminal pro–B-type natriuretic peptide

ROC = receiver-operating characteristic

SSA = senile systemic amyloidosis

^{99m}Tc-DPD = technetium-99m–3,3-diphosphono-1,2-propanodicarboxylic acid

TTR = transthyretin

TTR-FAC = transthyretin familial amyloidotic cardiomyopathy

WBR = whole-body retention

Figure 1. Representative Image of a Whole-Body Scan by ^{99m}Tc-DPD Scintigraphy

Detection of technetium-99m–3,3-diphosphono-1,2-propanodicarboxylic acid (^{99m}Tc-DPD) heart retention in a patient with a Val20Ile variant of the transthyretin gene.

were averaged over 3 consecutive cardiac cycles. In patients who were in atrial fibrillation, 5 consecutive beats were averaged. LV and right ventricular longitudinal function was assessed from the apical 4-chamber view by mitral annular plane systolic excursion (MAPSE) and tricuspid annular plane systolic excursion (TAPSE) by measuring the maximal excursion of the lateral site of the annulus after ventricular systole by M-mode imaging. Pulsed-wave tissue Doppler imaging of the mitral annulus was performed using a standard spectral Doppler sample volume gate length of 0.17 cm. The sample volume was placed on the medial mitral annulus in the apical 4-chamber view to measure mitral annular systolic velocity. LV hypertrophy index was calculated as the mean of the septal and posterior wall divided by one-half of LV end-diastolic diameter (normal range 0.33 to 0.41) (27).

^{99m}Tc-DPD scintigraphy. The procedure essentially followed the protocol described for the first time in 2002 (19). Preparation of ^{99m}Tc-DPD and quality control were carried out according to the procedures described by the manufacturer (CIS Bio International, Gif-sur-Yvette, France). For whole-body studies, a dual-head, whole-body gamma camera system (Siemens ECAM, Siemens Medical Systems, Hoffmann Estates, Illinois) was used.

The patients received 555 MBq ^{99m}Tc-DPD intravenously after urination. Whole-body scans were conducted both 5 min (soft-tissue phase) and 3 h (bone phase) after injection of ^{99m}Tc-DPD (Fig. 1). Tracer retention was assessed semi-quantitatively using a region-of-interest technique of planar images. All regions of interest were drawn by an independent investigator who was unaware of the patients' clinical data. The anterior image was copied to the posterior image and mirrored horizontally. The geometric mean of counts measured in the anterior and posterior projections was used in all further calculations. All regions of interest were corrected for background activity. Rectangular regions of interest were placed over the heart in the first scan and copied to the images obtained 3 h after injection. Irregular regions of interest were drawn over the bladder and urinary tract in the early and late images. Total registered counts in the whole-body region of interest at 5 min after injection were assumed to represent total injected activity. Counts in the whole-body region of interest at 3 h after injection, after subtraction of counts in bladder and urinary tract and normalization for scan speed, were decay corrected and compared with this value, resulting in the percentage of whole-body tracer retention (WBR). Counts in the heart region of interest at 3 h after injection were decay corrected and compared with whole-body counts at 5 min, indicating the relative percentage of tracer retention in the heart, sternum, and thoracic spine (HR).

Cardiac magnetic resonance. CMR was performed on a 1.5-T whole-body MRI scanner (Achieva, Philips Medical Systems, Best, the Netherlands), as described previously (28). In brief, resting LV function was determined by standard steady-state free-precession cine images in short axes, 2-, 3-, and 4-chamber views. Late gadolinium contrast agent (0.2 mmol/kg body weight) (Magnevist, Bayer-Schering-Pharma, Berlin, Germany) was administered if the estimated glomerular filtration rate was >30 ml/(min $\times$ 1.73 m^2) (n = 67). All data were analyzed in a blinded fashion by consensus reading (F.S., H.S.). Short-axis LV parameters were end-diastolic and -systolic volumes, ejection fraction, stroke volume, and LV myocardial mass. Longitudinal function was assessed by MAPSE and TAPSE. Regional LV wall thickness was analyzed in a modified American Heart Association-16 segment model. Late gadolinium enhancement was analyzed semi-quantitatively (0 = absent, 1 = mild, 2 = moderate,

3 = severe) in each of the 16 LV segments. Finally, the sum of contrast-enhanced CMR intensity of all 16 segments was calculated to express global contrast-enhanced CMR intensity (minimal = 0, maximal = 48).

Statistical analysis. Continuous data were expressed as median (interquartile range). Categorical variables were expressed as absolute numbers (percentage). Data were compared between TTR-FAC and SSA using the Mann-Whitney *U* or Fisher exact test. Correlation analyses were performed using the Spearman coefficient. Cutoff values for all-cause mortality and diagnosis of cardiac involvement by scintigraphy were determined by receiver-operating characteristic (ROC) analysis. Kaplan-Meier curves plotted for cumulative all-cause mortality of patients with cardiac amyloidosis (time between scintigraphy and death) were analyzed using log-rank analysis with right censoring. Using univariable and multivariable Cox regression models, the association of parameters assessed by CMR, echocardiography, electrocardiography, and laboratory analysis with all-cause mortality were investigated. A stepwise forward selection method was used for the entry and retention of variables in the Cox proportional hazard regression model, with all cause-mortality as a dependent variable and univariate risk factors as independent predictors (NT-proBNP, troponin T, and LV hypertrophy index). A separate analysis was performed in the subgroup of patients assessed by CMR. A p value <0.05 was considered statistically significant. Statistical analyses were performed using StatView version 5.0 (SAS Institute, Cary, North Carolina).

RESULTS

Of 70 patients, 60 presented with cardiac involvement. In 51 patients, cardiac involvement was proved by endomyocardial biopsy; 1 of these patients with a positive endomyocardial biopsy specimen did not meet noninvasive criteria of cardiac involvement (septal thickness of 10 mm). This patient had an HR of 2.9% and no late gadolinium enhancement by CMR. Some patients had clinical evidence of further involvement of the gut (n = 11), peripheral nerves (n = 20), lung (n = 4), vitreous body (n = 3), and urinary bladder (n = 2). Clinical, electrocardiographic, and echocardiographic characteristics of the study patients as well as the subgroup of patients with cardiac involvement are shown in detail in Table 1. Characteristics of the subgroup of patients assessed by CMR (n = 30) did not differ from the whole patient cohort (data not shown).

Scintigraphic findings. The median WBR of ^{99m}Tc-DPD was 79.6% (20.8%), median HR was 6.4% (3.2%), and median ratio of heart-to-whole body retention was 7.8% (3.9%). Comparison of scintigraphic parameters in the subgroup with SSA compared with TTR-FAC revealed no differences regarding HR, WBR, and heart-to-whole body ratio. WBR, HR, and heart-to-whole body ratio correlated well with morphological parameters (interventricular septum thickness, LV hypertrophy index) as well as with plasma levels of cardiac

Table 1. Clinical Demographics of the Patients With ATTR at Presentation

	All Patients (N = 70)	TTR-FAC (n = 36)	SSA (n = 34)	p Value	Cardiac Involvement (n = 60)
Male	53 (75.5)	20 (59)	33 (97)	<0.0001	47 (78)
Age, yrs	67.4 [16.9]	55.1 [17.1]	72.0 [4.8]	<0.0001	68.2 [18.8]
MBMI, kg/m^2 × g/l	1,104 [313]	1,060 [417]	1,183 [262]	0.0503	1,104 [299]
NYHA functional class					
I	16 (22.9)	14 (39.0)	2 (6.0)	0.0010	8 (13.3)
II	27 (38.6)	12 (33.0)	15 (44.0)	0.3537	25 (41.6)
III	26 (37.1)	10 (28.0)	16 (47.0)	0.0955	26 (43.3)
IV	1 (1.4)	0 (0.0)	1 (3.0)	NA	1 (1.7)
eGFR, ml/(min × 1.73 m^2)	71.1 [42.3]	93.8 [45.3]	62.3 [26.1]	<0.0001	75.1 [40.9]
Troponin T, µg/l	0.03 [0.045]	0.02 [0.03]	0.06 [0.09]	0.0007	0.04 [0.04]
NT-proBNP, ng/l	1,950 [3,982]	907 [2,081]	4,010.5 [3,725]	<0.0001	2,446 [3,452]
Sinus rhythm	53 (75.7)	32 (89.0)	21 (62.0)	0.0082	43 (71.7)
P-Q interval, ms	185 [50.0]	172 [42.0]	220 [52.5]	<0.0001	197 [52.0]
QRS duration, ms	106 [42.0]	96.5 [33.5]	116 [50.5]	0.0027	106 [26.5]
Low-voltage pattern	7 (10.0)	2 (6.0)	5 (15.0)	0.1462	6 (10.0)
IVS thickness, mm	17 [5.3]	16.0 [7.5]	20 [5.25]	0.0009	19 [5.0]
PW thickness, mm	16 [5.3]	14.5 [7.0]	17 [6]	0.0042	17 [6.0]
LVEDD, mm	43 [8.3]	43 [9.5]	43 [8.25]	0.8285	43 [7.75]
LVESD, mm	30 [7.5]	29 [8.0]	30 [6.5]	0.2526	30 [6.25]
MAPSE, mm	9.0 [6.0]	10.5 [5.3]	8 [3.3]	0.0006	10 [5.75]
TAPSE, mm	14.0 [7.5]	17.0 [6.5]	14 [6]	0.1286	14 [7.0]
MASV, m/s	3 [3.125]	6.5 [3.5]	5.5 [2.25]	0.0496	6 [2.0]
E/A ratio	1.49 [1.43]	1.45 [0.66]	2.5 [2.5]	0.0982	1.67 [2.12]
E/e′ ratio	12.3 [9.2]	11.1 [5.0]	13.3 [9.2]	0.0497	12.5 [9.1]
LV hypertrophy index*	0.80 [0.32]	0.73 [0.34]	0.85 [0.32]	0.0061	0.79 [0.25]
LV ejection fraction <40%	22 (31.4)	3 (8.0)	19 (56.0)	<0.0001	22 (36.7)

Values are n (%) or median [interquartile range]. *LV hypertrophy index was calculated as the mean of the septal and posterior wall divided by one-half of LV end-diastolic diameter (normal range 0.33 to 0.41) (27).
A = late diastolic transmitral flow velocity; ATTR = transthyretin amyloidosis; E = early diastolic transmitral flow velocity; e′ = tissue Doppler–derived early diastolic peak velocity at lateral mitral annulus; eGFR = estimated glomerular filtration rate according to the modification of diet in renal disease study; IVS = interventricular septum; LV = left ventricular; LVEDD = left ventricular end-diastolic diameter; LVESD = left ventricular end-systolic diameter; MAPSE = mitral annular plane systolic excursion; MASV = mitral annular systolic velocity; MBMI = modified body mass index (serum albumin × body mass index); NA = not applicable; NT-proBNP = N-terminal pro–B-type natriuretic peptide; NYHA = New York Heart Association; PW = posterior wall; SSA = senile systemic amyloidosis; TAPSE = tricuspid annular plane systolic excursion; TTR-FAC = transthyretin familial amyloid cardiomyopathy.

Table 2. Correlation of Scintigraphy and Clinical Parameters

	Whole-Body Retention		Heart Retention		Heart-to-Whole-Body Retention	
	r	p Value	r	p Value	r	p Value
IVS thickness	0.440	0.0002	0.533	<0.0001	0.405	0.0006
LV hypertrophy index*	0.425	0.0003	0.455	<0.0001	0.278	0.0206
Log troponin T	0.357	0.0032	0.549	<0.0001	0.447	0.0002
Log NT-proBNP	0.634	<0.0001	0.660	<0.0001	0.484	<0.0001
MASV	0.364	0.0021	0.526	<0.0001	0.442	0.0001
MAPSE	0.250	0.0379	0.470	<0.0001	0.413	0.0004
TAPSE	0.302	0.0125	0.326	0.0066	0.258	0.0333
eGFR	0.525	<0.0001	0.478	<0.0001	0.266	0.0263

*LV hypertrophy index was calculated as the mean of the septal and posterior wall divided by one-half of LV end-diastolic diameter (27).
Abbreviations as in Table 1.

biomarkers (troponin T, NT-proBNP). An inverse correlation of WBR, HR, and heart-to-whole body ratio was observed with functional parameters of amyloid burden (mitral annular systolic velocity, MAPSE, TAPSE) as well as renal function (Table 2). No correlation was observed with age and modified body mass index. The cutoff value of HR for diagnosis of cardiac involvement with highest sensitivity (80%) and specificity (90%) was 4.8% (area under the curve: 0.92 ± 0.04; 95% confidence interval: 0.84 to 0.99; $p < 0.0001$). In total, in 51 patients, HR above this cutoff was observed.

Late gadolinium enhancement was observed in 28 of 30 patients (93.3%) assessed by CMR. A significant correlation between the extent of late gadolinium enhancement by semiquantitative analysis with WBR ($r = 0.506$, $p = 0.0071$) as well as HR ($r = 0.407$, $p = 0.0350$) was observed. Late gadolinium enhancement correlated with troponin T ($r = 0.613$, $p < 0.0001$) and NT-proBNP ($r = 0.620$, $p = 0.0006$).

Survival analysis. Survival analysis was performed in the cohort of 60 patients with cardiac involvement. In total, 25 of 60 patients died during a median follow-up of 31.1 months (interquartile range: 31.3 months). Survival did not differ between patients with SSA and TTR-FAC ($p = 0.213$). All-cause mortality was worse in patients with an HR and heart-to-whole body ratio (but not WBR) above the median compared with patients with HR and heart-to-whole body ratio below the median (Fig. 2). Univariate Cox regression revealed NT-proBNP, troponin T, MAPSE, and LV hypertrophy index as predictors of outcome (Table 3). Based on these results, NT-proBNP, troponin T, and LV hypertrophy index were included in the multivariate Cox proportional hazards model with stepwise forward regression. By multivariate analysis, troponin T remained the only independent predictor of survival (hazard ratio: 4.4, $p < 0.05$). There was no collinearity between troponin T and NT-proBNP. A Kaplan-Meier curve for patients stratified by median of troponin T is shown in Figure 3. By ROC analysis, the troponin T cutoff value predicting all-cause mortality with highest sensitivity (80%) and specificity (68.7%) was 0.0375 μg/l (area under the curve: 0.746; 95% confidence interval: 0.612 to 0.880; $p = 0.002$). Cox regression analysis of the subgroup of patients assessed by CMR revealed troponin T as the only predictor of survival (hazard ratio: 10.5; $p < 0.05$). When scintigraphy variables were included in a multivariate model, none of them were independent predictors of survival.

DISCUSSION

Cardiac involvement represents the major complication in both hereditary ATTR and SSA (2,9,11). Noninvasive indicators of severity of ATTR and predictors of survival are limited. The most important finding of the present study is that ^{99m}Tc-DPD tracer retention correlates well with established parameters indicating severity of cardiac disease. For risk stratification, troponin T emerged as the only independent and powerful variable after adjustment for NT-proBNP and LV hypertrophy index.

Noninvasive diagnosis of cardiac ATTR. ^{99m}Tc-DPD scintigraphy is a simple diagnostic tool that is well established and widely available for skeletal imaging. A decade ago, it was shown that this tool was capable of identifying (cardiac) TTR amyloid deposition by increased tracer retention (19).

In recent years, high sensitivity and specificity for the detection of (cardiac) ATTR were demonstrated by ^{99m}Tc-DPD scintigraphy (29). Finally, minor tracer retention was reported in patients with light-chain amyloidosis and advanced cardiac involvement (30). Thus, it was concluded that absence of cardiac tracer retention is almost pathognomonic for light-chain amyloidosis, whereas the presence of severe tracer retention is almost pathognomonic for ATTR. Moreover, cardiac tracer retention can be an incidental finding if skeletal imaging is performed in older patients primarily to detect any skeletal abnormality. The precise mechanism of bisphosphonate binding to amyloid remained unclear, but a high calcium load in amyloid tissue was suggested to be causative (31).

Although an age-dependent increase in tracer retention may be suspected, no correlation of WBR and HR with age was observed in this study. This may be explained by the wide heterogeneity of phenotypes in ATTR, with age at onset of amyloid deposition ranging between 30 and 60 years and the fact that almost one-half of the present patient cohort consists of SSA patients with a mean age of 72.3 years.

Recently, in a smaller study consisting of 20 patients with 3 different variants of the TTR gene (*Glu89Gln*, *Phe64Leu*, and *Thr49Ala*), it was demonstrated that detection of cardiac amyloid deposition was more extensive and sensitive when assessed by HR of ^{99m}Tc-DPD rather than by late gadolinium enhancement (32). Even though these variants were associated with polyneuropathy, cardiomyopathy, and carpal tunnel ligament syndrome, HR was present in one-half of the patients. According to these reports, this noninvasive tool was increasingly used specifically as a surrogate for cardiac amyloid load. However, detailed diagnostic criteria for cardiac involvement have not been reported previously.

In a previous study by Rapezzi et al. (30), comparison of mean values of ^{99m}Tc-DPD HR between patients with TTR-related cardiac amyloidosis, light-chain related cardiac amyloidosis, and controls was performed. The same is true for the study of Bokhari et al. (33) comparing mean heart-to-contralateral ratio of technetium-99m pyrophosphate retention according to the subtypes of amyloidosis, namely, light chain, mutant, as well as wild-type ATTR. However, none of the studies referred to a cutoff value of HR defining cardiac involvement. Thus, to the best of our knowledge, this is the first study reporting a ROC-derived cutoff value for the definition of cardiac involvement in ATTR. An HR of 4.8% indicated cardiac involvement with an acceptable sensitivity (80%) and specificity (90%).

Risk prediction of ATTR. Risk assessment in patients with cardiac amyloidosis is crucial in clinical care. Almost all strategies by electrocardiography and echocardiography were derived in patients with light-chain amyloidosis (15–18,34,35). Due to the diversity of light-chain amyloidosis and ATTR, indicators established in light-chain amyloidosis may not apply to ATTR (12,36,37). Moreover, due to the high specificity of ^{99m}Tc-DPD for cardiac ATTR, this tool may have a potential impact on risk assessment. At present, data on risk prediction by echocardiography, cardiac biomarkers, CMR, and ^{99m}Tc-DPD scintigraphy in ATTR are limited.

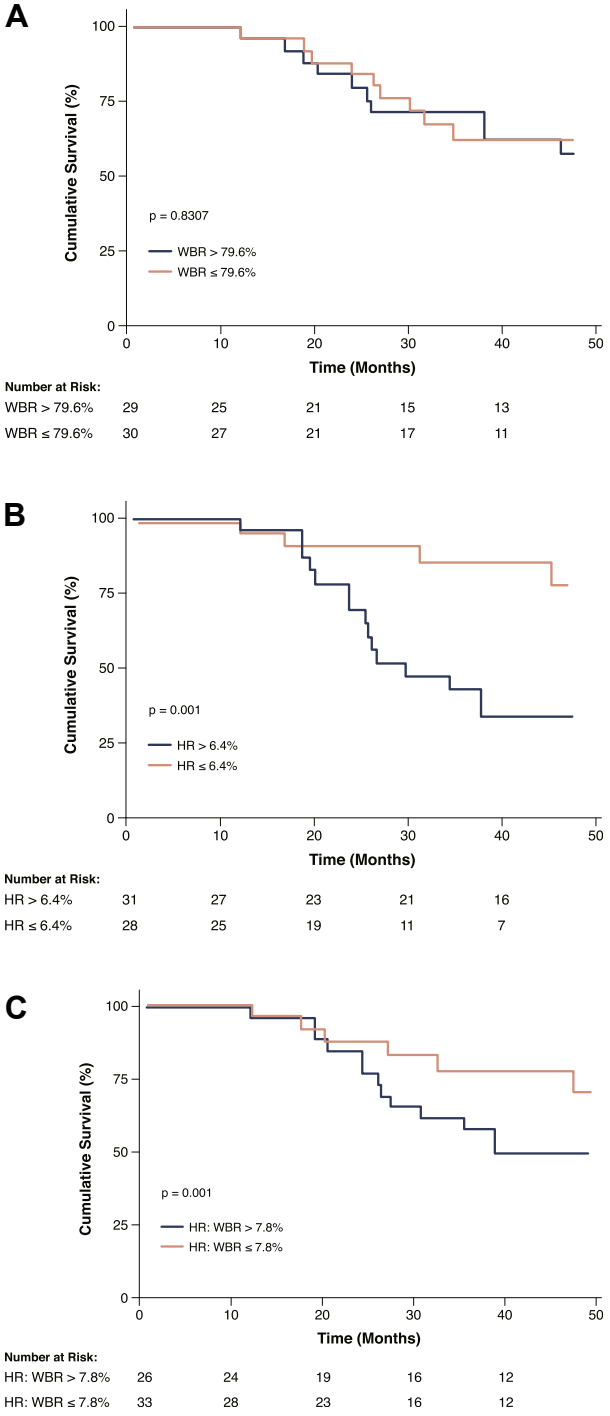

Figure 2. Survival Analysis According to Scintigraphy Findings

Association of median of whole-body retention (WBR) **(A)**, heart, sternum, and thoracic spine tracer retention (HR) **(B)**, and ratio of HR to WBR (HR:WBR) **(C)** with survival.

Although we were able to observe correlations of different morphological and functional parameters assessed by echocardiography and ^{99m}Tc-DPD

Table 3. Results of Univariate Cox Regression Analysis to Determine Death in the Whole Patient Cohort

	p Value	Hazard Ratio	95% Confidence Interval
Whole-body retention	0.8089	1.31	0.15–11.64
Heart retention	0.0702	15.31	0.80–293.61
Heart to whole body	0.0725	13.40	0.78–304.30
Sex	0.3361	0.62	0.23–1.65
MBMI	0.4487	1.00	1.00–1.00
Age	0.1687	1.03	0.99–1.07
Atrial fibrillation	0.0836	2.06	0.91–4.68
QRS width	0.7471	1.01	0.99–1.01
IVS thickness	0.2225	1.06	0.97–1.17
LV hypertrophy index*	0.0235	6.12	1.28–29.32
E/e′	0.7868	0.99	0.95–1.04
E/A	0.7907	0.95	0.63–1.43
MAPSE	0.0167	0.85	0.74–0.97
TAPSE	0.1290	0.95	0.88–1.02
MASV	0.2322	0.85	0.66–1.11
eGFR	0.0927	0.99	0.97–1.00
Log NT-proBNP	0.0287	2.83	1.11–7.17
Log troponin T	0.0006	7.25	2.35–22.38

*LV hypertrophy index was calculated as the mean of the septal and posterior wall divided by one-half of the LV end-diastolic diameter (27).
Abbreviations as in Table 1.

scintigraphy that were associated with the outcome of ATTR, by multivariate analysis, troponin T remained the only independent predictor of survival. This appears to be in contrast to a recent report from Rapezzi et al. (38) summarizing 63 ATTR patients with a median follow-up of 14 months,

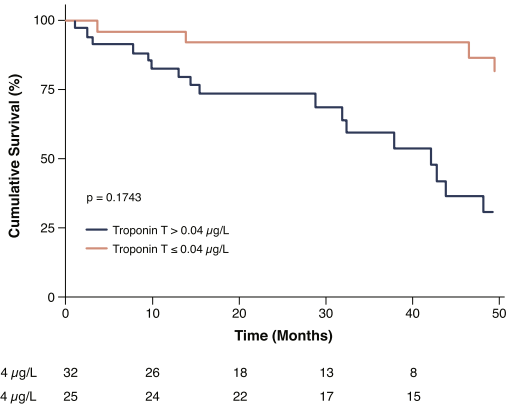

Figure 3. Survival Analysis According to Troponin T

Association of troponin T plasma level with survival stratified by the median value.

which demonstrated age and filling pattern as independent predictors of a combined endpoint of death from cardiovascular causes (fatal arrhythmias or severe worsening of heart failure), hospital stay due to congestive heart failure, complete atrioventricular block, atrial fibrillation/flutter, myocardial infarction, or stroke. Information on predictors of death in this study is lacking. There were only 2 deaths reported during follow-up. In a small cohort of patients with wild-type ATTR, a decrease in longitudinal myocardial function indicated by MAPSE was predictive of survival (13). A previous report on 34 patients (some with light-chain amyloidosis, some with ATTR) revealed LV fraction by CMR and NT-proBNP as independent predictors of survival (28), but subgroup analysis of light-chain amyloidosis or ATTR was not performed.

In light-chain amyloidosis, increased levels of troponin and NT-proBNP have been well established as predictors of poor outcome (16,17). Troponin T elevation has been shown to correlate with a more aggressive disease and a shorter survival (17,39), whereas NT-proBNP is helpful to assess response to treatment (16). Both NT-proBNP and troponins have been incorporated in a risk score protocol widely used in clinical practice (40).

In a recent report on the use of cardiac biomarkers (troponin T and I and B-type natriuretic peptide) in late-onset Val30Met patients, neither troponin T nor I was a surrogate for the presence of cardiac amyloidosis as detected by echocardiography (41). In these patients, abnormal values of B-type natriuretic peptide were early indicators of heart failure already present despite normal strain values by echocardiography.

Study limitations. In the present study, a subgroup of 30 patients was assessed by CMR. Although this is a small patient cohort, it is by far a well-sized number of patients with ATTR (28,42). Interestingly, troponin T correlated well with the extent of late gadolinium enhancement. Both troponin T and late gadolinium enhancement are indicators of myocardial damage, suggesting a potential impact of late gadolinium enhancement on outcome; however, this needs to be evaluated in a larger patient cohort. As ^{99m}Tc scans impose an effective radiation dose of approximately 3 mSv, its diagnostic use needs to be compared with T1 mapping by CMR recently reported as a noninvasive diagnostic tool for diagnosis of cardiac amyloidosis (42).

In summary, ^{99m}Tc-DPD scintigraphy appears to be a useful tool for noninvasive diagnosis of ATTR (especially wild type) if cardiac biopsy is to be avoided and if amyloid was established by

histology in any extracardiac organ. Nevertheless, the prognostic value of ^{99m}Tc-DPD scintigraphy appears to be limited.

CONCLUSIONS

In recent reports, it was demonstrated that ^{99m}Tc-DPD scintigraphy plays an important role for the (differential) diagnosis of cardiac ATTR. In the present report, it was demonstrated that quantitative analysis of tracer retention relates to cardiac involvement in ATTR; however, by multivariate analysis, troponin T remained the only independent predictor of all-cause mortality.

Reprint requests and correspondence: Dr. Arnt V. Kristen, Department of Cardiology, Angiology, and Respiratory Medicine, University Hospital Heidelberg, Im Neuenheimer Feld 410, D-69120 Heidelberg, Germany. *E-mail: Arnt.Kristen@med.uni-heidelberg.de.*

REFERENCES

1. Coelho T, Maurer MS, Suhr OB. THAOS—The Transthyretin Amyloidosis Outcomes Survey: initial report on clinical manifestations in patients with hereditary and wild-type transthyretin amyloidosis. Curr Med Res Opin 2013;29:63–76.
2. Rapezzi C, Longhi S, Milandri A, et al. Cardiac involvement in hereditary-transthyretin related amyloidosis. Amyloid 2012;19:16–21.
3. Ihse E, Ybo A, Suhr O, Lindqvist P, Backman C, Westermark P. Amyloid fibril composition is related to the phenotype of hereditary transthyretin V30M amyloidosis. J Pathol 2008;216:253–61.
4. Hund E, Linke RP, Willig F, Grau A. Transthyretin-associated neuropathic amyloidosis. Pathogenesis and treatment. Neurology 2001;56:431–5.
5. Saraiva MJ. Hereditary transthyretin amyloidosis: molecular basis and therapeutical strategies. Expert Rev Mol Med 2002;4:1–11.
6. Ando Y, Nakamura M, Araki S. Transthyretin-related familial amyloidotic polyneuropathy. Arch Neurol 2005;62:1057–62.
7. Connors LH, Doros G, Sam F, Badiee A, Seldin DC, Skinner M. Clinical features and survival in senile systemic amyloidosis: comparison to familial transthyretin cardiomyopathy. Amyloid 2011;18 Suppl 1:152–4.
8. Benson MD. Pathogenesis of transthyretin amyloidosis. Amyloid 2012;19:14–5.
9. Dungu JN, Anderson LJ, Whelan CJ, Hawkins PN. Cardiac transthyretin amyloidosis. Heart 2012;98:1546–54.
10. Cornwell GG III, Murdoch WL, Kyle RA, Westermark P, Pitkanen P. Frequency and distribution of senile cardiovascular amyloid. A clinicopathologic correlation. Am J Med 1983;75:618–23.
11. Ruberg FL, Berk JL. Transthyretin (TTR) cardiac amyloidosis. Circulation 2012;126:1286–300.
12. Rapezzi C, Merlini G, Quarta CC, et al. Systemic cardiac amyloidoses: disease profiles and clinical courses of the 3 main types. Circulation 2009;120:1203–12.
13. Kristen AV, Haufe S, Schonland SO, et al. Skeletal scintigraphy indicates disease severity of cardiac involvement in patients with senile systemic amyloidosis. Int J Cardiol 2011;164:179–84.
14. Suhr OB, Ericzon BG. Selection of hereditary transthyretin amyloid patients for liver transplantation: the Swedish experience. Amyloid 2012;19 Suppl 1:78–80.
15. Kristen AV, Perz JB, Schonland SO, et al. Rapid progression of left ventricular wall thickness predicts mortality in cardiac light-chain amyloidosis. J Heart Lung Transplant 2007;26:1313–9.
16. Palladini G, Campana C, Klersy C, et al. Serum N-terminal pro-brain natriuretic peptide is a sensitive marker of myocardial dysfunction in AL amyloidosis. Circulation 2003;107:2440–5.
17. Dispenzieri A, Kyle RA, Gertz MA, et al. Survival in patients with primary systemic amyloidosis and raised serum cardiac troponins. Lancet 2003;361:1787–9.
18. Kristen AV, Perz J, Schonland S, et al. Non-invasive predictors of survival in cardiac amyloidosis. Eur J Heart Fail 2007;9:617–24.
19. Puille M, Altland K, Linke RP, et al. 99mTc-DPD scintigraphy in transthyretin-related familial amyloidotic polyneuropathy. Eur J Nucl Med Mol Imaging 2002;29:376–9.
20. Perugini E, Guidalotti PL, Salvi F, et al. Noninvasive etiologic diagnosis of cardiac amyloidosis using 99mTc-3,3-diphosphono-1,2-propanodicarboxylic acid scintigraphy. J Am Coll Cardiol 2005;46:1076–84.
21. Glaudemans AW, Slart RH, Zeebregts CJ, et al. Nuclear imaging in cardiac amyloidosis. Eur J Nucl Med Mol Imaging 2009;36:702–14.
22. Altland K, Benson MD, Costello CE, et al. Genetic microheterogeneity of human transthyretin detected by IEF. Electrophoresis 2007;28:2053–64.
23. Gertz MA, Comenzo R, Falk RH, et al. Definition of organ involvement and treatment response in immunoglobulin light chain amyloidosis (AL): a consensus opinion from the 10th International Symposium on Amyloid and Amyloidosis. Am J Hematol 2005;79:319–28.
24. Khouri SJ, Maly GT, Suh DD, Walsh TE. A practical approach to the echocardiographic evaluation of diastolic function. J Am Soc Echocardiogr 2004;17:290–7.
25. Lang RM, Bierig M, Devereux RB, et al. Recommendations for chamber quantification: a report from the American Society of Echocardiography's Guidelines and Standards Committee and the Chamber Quantification Writing Group, developed in conjunction with the European Association of Echocardiography, a branch of the European Society of Cardiology. J Am Soc Echocardiogr 2005;18:1440–63.
26. Nagueh SF, Appleton CP, Gillebert TC, et al. Recommendations for the evaluation of left ventricular diastolic function by echocardiography. Eur J Echocardiogr 2009;10:165–93.
27. Reichek N, Devereux RB. Reliable estimation of peak left ventricular systolic pressure by M-mode echographic-determined end-diastolic relative wall thickness: identification of severe valvular aortic stenosis in adult patients. Am Heart J 1982;103:202–3.
28. Lehrke S, Steen H, Kristen AV, et al. Serum levels of NT-proBNP as surrogate for cardiac amyloid burden: new evidence from gadolinium-enhanced cardiac magnetic resonance imaging in patients with amyloidosis. Amyloid 2009;16:187–95.

29. Rapezzi C, Guidalotti P, Salvi F, Riva L, Perugini E. Usefulness of 99mTc-DPD scintigraphy in cardiac amyloidosis. J Am Coll Cardiol 2008; 51:1509–10.
30. Rapezzi C, Quarta CC, Guidalotti PL, et al. Usefulness and limitations of 99mTc-3,3-diphosphono-1,2-propanodicarboxylic acid scintigraphy in the aetiological diagnosis of amyloidotic cardiomyopathy. Eur J Nucl Med Mol Imaging 2011;38:470–8.
31. Yood RA, Skinner M, Cohen AS, Lee VW. Soft tissue uptake of bone seeking radionuclide in amyloidosis. J Rheumatol 1981;8:760–6.
32. Minutoli F, Di Bella G, Mazzeo A, et al. Comparison between (99m) Tc-diphosphonate imaging and MRI with late gadolinium enhancement in evaluating cardiac involvement in patients with transthyretin familial amyloid polyneuropathy. AJR Am J Roentgenol 2013;200: W256–65.
33. Bokhari S, Castano A, Pzniakoff T, et al. 99mTc-pyrophosphate scintigraphy for differentiating light-chain cardiac amyloidosis from the transthyretin-related familial and senile cardiac amyloidosis. Circ Cardiovasc Imaging 2013;6:195–201.
34. Palladini G, Malamani G, Co F, et al. Holter monitoring in AL amyloidosis: prognostic implications. Pacing Clin Electrophysiol 2001;24:1228–33.
35. Bellavia D, Pellikka PA, Abraham TP, et al. 'Hypersynchronisation' by tissue velocity imaging in patients with cardiac amyloidosis. Heart 2009;95: 234–40.
36. Ng B, Connors LH, Davidoff R, Skinner M, Falk RH. Senile systemic amyloidosis presenting with heart failure: a comparison with light chain-associated amyloidosis. Arch Intern Med 2005;165:1425–9.
37. Kyle RA, Spittell PC, Gertz MA, et al. The premortem recognition of systemic senile amyloidosis with cardiac involvement. Am J Med 1996; 101:395–400.
38. Rapezzi C, Quarta CC, Guidalotti PL, et al. Role of (99m) Tc-DPD scintigraphy in diagnosis and prognosis of hereditary transthyretin-related cardiac amyloidosis. J Am Coll Cardiol Img 2011;4:659–70.
39. Kristen AV, Giannitsis E, Lehrke S, et al. Assessment of disease severity and outcome in patients with systemic light-chain amyloidosis by the high-sensitivity troponin-T assay. Blood 2010;116:2455–61.
40. Dispenzieri A, Gertz MA, Kyle RA, et al. Serum cardiac troponins and N-terminal pro-brain natriuretic peptide: a staging system for primary systemic amyloidosis. J Clin Oncol 2004; 22:3751–7.
41. Suhr OB, Anan I, Backman C, et al. Do troponin and B-natriuretic peptide detect cardiomyopathy in transthyretin amyloidosis? J Intern Med 2007;263: 294–301.
42. Fontana M, Banypersad SM, Treibel TA, et al. Native t1 mapping in transthyretin amyloidosis. J Am Coll Cardiol Img 2014;7:57–65.

Key Words: cardiac magnetic resonance ■ echocardiography ■ skeletal scintigraphy ■ survival ■ transthyretin amyloidosis.